ELSEVIER

Journal of Nuclear Materials 295 (2001) 49–56

journal of nuclear materials

www.elsevier.nl/locate/jnucmat

Hydrogen isotope diffusive transport parameters in pure polycrystalline tungsten

G.A. Esteban *, A. Perujo, L.A. Sedano [1], K. Douglas

European Commission Joint Research Center, Environment Institute, T.P. 680, 21020 Ispra (VA), Italy

Received 9 November 2000; accepted 2 February 2001

Abstract

An experimental time-dependent isovolumetric gas-phase desorption technique has been used to obtain the diffusive transport parameters diffusivity (D), Sieverts' constant (K_s) and permeability (Φ) as well as the trapping parameters trap site concentration (N_t) and trapping energy (E_t) of hydrogen isotopes (protium and deuterium) in tungsten. The study was performed in the 673 to 1073 K temperature range and with driving pressures from 1.3×10^4 to 10^5 Pa. The characteristic protium oscillation temperatures in the ground state $\theta = 893$ K and in the excited state $\theta^* = 2467$ K were calculated using the approximation of the ideal harmonic vibration of hydrogen isotope atoms in a unique type of solution site. The extrapolated tritium transport parameters obtained using these oscillation temperatures were: D ($m^2\ s^{-1}$) $= 5.34 \times 10^{-10} \exp(-11.2/RT)$, K_s (mol m^{-3} $Pa^{-1/2}$) $= 2.25 \times 10^{-2} \exp(-27.8/RT)$, Φ (mol m^{-1} $Pa^{-1/2}$ s^{-1}) $= 1.20 \times 10^{-11} \exp(-3.9/RT)$, E_t (kJ mol^{-1}) $= 100.5$, N_t (sites m^{-3}) $= 2.3 \times 10^{23}$.

1. Introduction

Besides other refractory materials, tungsten (W) has been identified as a suitable candidate plasma facing material for limiters and divertors of thermonuclear fusion reactors [1,2]. The excellent thermomechanical and physical properties of W (good thermal conductivity, high temperature strength, high energy threshold for physical sputtering, high melting point and low vapour pressure) makes it very attractive for its consideration as plasma facing high heat flux material. Furthermore, W does not form hydrides or co-deposits with tritium (H_T) at reference fusion wall operating conditions. The characterisation of the behaviour of the hydrogen (H) isotopes transport in W is needed in order to quantify major fusion reactor design issues as safety, breeding feasibility, fuel economy and plasma stability. The slow transport kinetics of H isotopes in W make the experimental measurement of the H transport parameters arduous (long measurement times may be required and a certain measuring accuracy must be assured in order to avoid background noise). This feature is probably responsible for the lack of reliable H transport data in W. The existing results [3–6] show an enormous dispersion.

This work reports the results from an isovolumetric gas-phase desorption experiment (IDE) undertaken with protium (H_P) and deuterium (H_D) in W, in the temperature range from 673 to 1073 K and gas partial pressures from 1.3×10^4 to 10^5 Pa. The diffusive transport parameters (permeability Φ, effective diffusivity D_{eff} and effective Sieverts' constant $K_{s,eff}$) and the trapping parameters (the trap density N_t and the trapping activation energy E_t) of the H isotopes are obtained.

2. Review of existing data

Table 1 reports the main H diffusive transport data in W available in the literature [3–9]; the lattice Sieverts'

* Corresponding author. Present address: U.P.V – E.T.S.I.I.T., Dpt. Ingeniería Nucl. y Mec. de Fluidos, Alda. Urquijo, s/n, 48013 Bilbao, Spain. Tel.: +39-94 601 4043; fax: +39-94 601 4159.

E-mail address: inpesalg@bi.ehu.es (G.A. Esteban).

[1] Present address: CIEMAT, Dpt. Imp. Ambiental de la Energía, Avda. Complutense 28040, Madrid (Spain).

0022-3115/01/$ - see front matter
PII: S0022-3115(01)00486-X

Table 1
Experimental Sieverts' constants (K_{s0}, pre-exponential, E_s, solution energy), diffusivities (D_0, pre-exponential, E_d, diffusion energy) and trapping parameters (N_t, trapping site density, E_t, trapping energy) of hydrogen in tungsten

Material	K_{s0} (mol m^{-3} Pa$^{-1/2}$)	E_s (kJ mol^{-1})	D_0 (m^2 s^{-1})	E_d (kJ mol^{-1})	T (K)	Ref.
Sintered and rolled cylinder	1.48	101.0	4.1×10^{-7}	37.7	1100–2400	[3]
Filament ribbon	1039 (at 2713 K)	267.9	7.2×10^{-8}	173.7	1510–1902	[4]
Poly and monocrystalline W tubes	1.22×10^{-4}	2.9	6.0×10^{-4}	103.4	400–1200	[5]
1 mm diameter commercial wire	–	–	8.1×10^{-6}	82.9	1055–1570	[6]
Single crystal	–	–	3.0×10^{-10}	24.1	300–900	
Wrought	–	–	1.5×10^{-10}	24.1	300–900	[7]
	E_t (kJ mol^{-1})	N_t (sites m^{-3})				
Single crystal						
Natural traps	48.2	3.8×10^{26}				
Ion induced (1.5, 8 keV D^+)	120.6	1.0×10^{28}			300–900	[7]
Wrought						
Natural traps	48.2	6.3×10^{26}				
Pure W rolled 0.3 mm foil						
Weak defects	53.0	–			350–750	[8]
Ion induced (1.5, 8 keV D^+)	96.5	–				
Polycrystalline						
Unannealed	150.5	4.4×10^{24}				
Annealed at 1273 K	137.0	1.6×10^{24}			610–823	[9]
Annealed at 1673 K	129.3	8.2×10^{23}				

constant and diffusivity pre-exponentials K_{s0} and D_0 and the respective activation energies for solution (E_s) and diffusion (E_d) are tabulated together with the characteristic trapping parameters (the trap density N_t and the trapping energy E_t).

Frauenfelder [3] modelled the H degassing from a previously loaded specimen obtaining the H diffusivity and solubility in rolled sintered W (gas loading pressure 8×10^4 Pa and temperatures between 1100 and 2400 K). The use of the gas evolution technique in [3] presents some accuracy drawbacks: (1) the neglect of H desorbed and pumped-out from the specimen between loading and release phases and (2) the ('3 min') transient flash heating to reach the desired constant temperature level. Moore and Unterwald [4] evaluated the H transport parameters in a hot W filament (1200–2500 K) studying the atomisation phenomenon of hydrogen molecules. Zakharov and Sharapov [5] measured the permeation of H through a tube of tungsten (with a sealed end) from 673 to 1473 K and pressures from 1.3×10^2 to 2.6×10^4 Pa. The specimen was polycrystalline W and was manufactured by vapour–gas phase W hexafluoride reduction. Ryabchikov [6] modelled the H degassing rates of previously up-to-saturation loaded commercial wires, evaluating diffusivities in the temperature range 1055–1570 K. Franzen et al. [7] modelled the H trapping in and release from specimens previously implanted with H^+. They studied two types of W specimen, single crystal and wrought, in the temperature range 300–900 K obtaining the H diffusivity and characterising the trapping phenomenon for differentiated natural and ion-induced traps. An analogous work on the trapping characteristics was developed by Pisarev et al. [8] studying ion implantation of H_D in tungsten from 350 to 750 K. From the thermodesorption peak analysis two activation energies for trapping were evaluated. Anderl et al. [9] used an ion driven permeation technique in polycrystalline W to study H_D transport and trapping phenomena. They used diverse specimens of the same material (polycrystalline tungsten foils manufactured by powder metallurgy) annealed at different temperatures. They noticed the effect of the heat treatment, i.e., the microstructure configuration, on the trapping energy.

3. Experimental

3.1. Specimens

The sample material was pure unalloyed polycrystalline W. The specimens consisted of four cylinders with 6 mm diameter and 60 mm height. The specimen dimensions were defined in this manner to make feasible the H transport study using the approximation to an

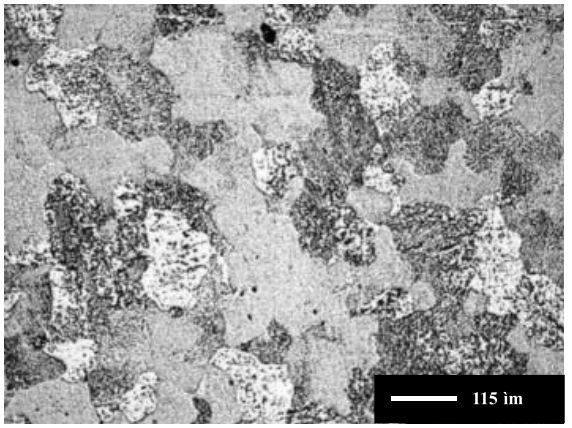

Fig. 1. Optical micrograph of the 'as-received' tungsten used in the experiment.

infinite long cylinder geometry. The specimens were cut by means of spark erosion from a rod (6 mm diameter) of material containing a minimum of 99.98% W. Each batch tested consisted of four specimens to provide a larger signal-to-noise ratio for the experiments. The specimens were used as-received without any heat treatment. Fig. 1 shows the polycrystalline microstructure of the material.

In order to remove residual oxides, the specimens were etched in a 20% KOH solution. Subsequently, the surface was mechanically polished and degreased. Finally, the specimens were dried in a vacuum furnace (100°C) before insertion into the experimental rig. These processes eliminate any impurity left on the surface that might affect the penetration of H into the bulk of the material.

3.2. Measuring procedure

The details for the IDE rig and measuring procedure are given elsewhere [10–12]. The specimens are placed in the measuring chamber having a constant volume. The chamber is loaded (loading phase), not necessarily up to saturation, at given hydrogen pressure and temperature for a time τ_l. During a short time τ_p, the fast pumping of the chamber (pumping phase) induces the hydrogen release from the specimens to the chamber (release phase).

A single experimental measurement (Fig. 2) consists in the recording of the pressure signal for the release period τ_r. Each measurement is followed by a blank run, under the same experimental conditions, (i.e., same loading pressure, specimens temperature and times τ_l, τ_p, τ_r), without specimens, to account for the contribution of the inner wall outgassing of the experimental vessel. The 'net' pressure release curve is then obtained by point-to-point pressure subtraction. This procedure must be performed at each experimental temperature in order not to evaluate erroneous transport parameters produced by the wall-outgassing.

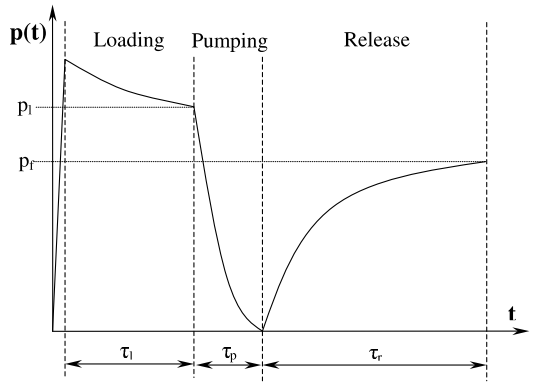

Fig. 2. Experimental phases in a single isovolumetric desorption run. The pressure $p(t)$ and time scales are different for each phase in order to appreciate their pressure profiles; τ_l, τ_p and τ_r are loading, pumping and release times, respectively; p_l and p_f the pressures measured in the experimental chamber at the end of the loading and release phases, respectively.

4. Modelling

At high working temperatures, hydrogen in W exhibits a very low solubility and slow migration kinetics (Fig. 3). Consequently, in order to avoid very long cost-effective experimental times and stability problems in the measuring devices, non-stationary models are used [13,14]. The release rate model solves the diffusion equation in an infinite cylinder geometry linking all the three phases (loading, pumping and release) and provides transient gas concentration profiles for each single phase (Fig. 4).

The effective transport parameters D_{eff} and $K_{s,eff}$ are evaluated for each experimental temperature using a

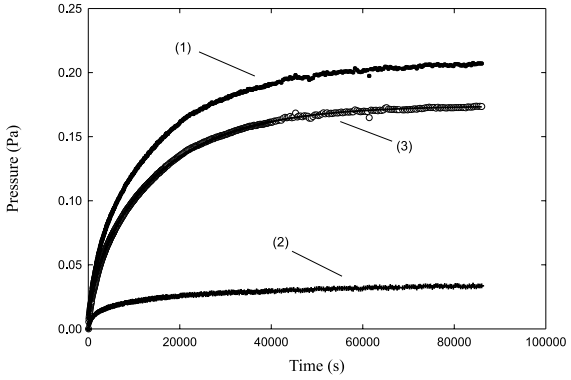

Fig. 3. Pressure increase in an experimental measurement: (1) run with specimens, (2) blank run, (3) effective pressure increase and fitting.

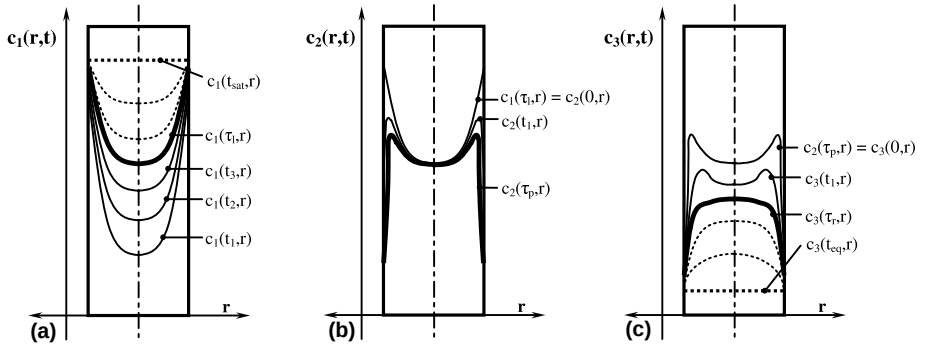

Fig. 4. Hydrogen concentration $c_i(r,t)$ profiles in a non-stationary sequence of the three experimental phases: (a) loading phase; (b) pumping phase; (c) release phase. The concentration profiles presented by solid lines show the evolution of concentration with time during each phase; the thick lines indicate the profile attained at the end of each phase; the dashed lines show the progression the concentration profiles would follow till equilibrium situation in case of long enough time allowed.

non-linear least squares fitting of the theoretical H pressure increase to the pressure increase measured in the experimental chamber (Fig. 3). The theoretical expression for the measured pressure is obtained from the non-stationary solution of radial Fick's second law in the three phases; the same mathematical development proposed in [13] but in the absence of surface effects:

$$p(t) = \frac{RT}{(V-4V_s)} 4\pi h \sum_{n=1}^{\infty} \frac{1}{\alpha_n^2} \left[1-\exp\left(-D_{\mathrm{eff}}\alpha_n^2 t\right)\right] \times \left\{c_L\left[1-\exp\left(-D_{\mathrm{eff}}\alpha_n^2\tau_l\right)\right]\exp\left(-D_{\mathrm{eff}}\alpha_n^2\tau_p\right) - c_f\right\}, \quad (1)$$

where V_s is the volume of one of the four identical specimens measured simultaneously, V the volume of the experimental chamber, h the height of the specimens. α_n (m^{-1}) (where $n = 1, 2, \ldots$) are the infinite real roots of the equation $J_0(a\alpha_n) = 0$, a is the cylinder radius. c_L and c_f are the H concentration at the sub-surface of the cylindrical specimens during the loading phase and at the end of the release phase, respectively; once the atomic transport is verified, they can be evaluated by means of Sieverts' law $c_L = K_{s,\mathrm{eff}} \times p_l^{1/2}$ and $c_f = K_{s,\mathrm{eff}} \times p_f^{1/2}$, p_l being the loading pressure and p_f the final pressure at the end of the release phase.

The effective transport parameters are affected by the trapping phenomenon [15] that increases the absorbed gas inventory and slows the transport kinetics following the well-known relations [16]:

$$K_s = K_{s,0}\exp(-E_s/RT),$$
$$K_{s,\mathrm{eff}} = K_s(1+(N_t/N_l)\exp(E_t/RT)),$$
$$D = D_0\exp(-E_d/RT),$$
$$D_{\mathrm{eff}} = D/(1+(N_t/N_l)\exp(E_t/RT)),$$

D and K_s being the diffusivity and the Sieverts' constant characteristic of the lattice, D_0 and K_{s0} their respective pre-exponentials. E_d, E_s are the diffusion and solution energies, N_l (m^{-3}) the lattice dissolution sites concentration, N_t (m^{-3}) the trap sites concentration and E_t the trapping energy.

W shows a body-centred cubic structure and H accommodates preferentially in the tetrahedral interstitial positions similar to α-Fe [17]. Consequently, the density of the solution sites into the lattice is $N_l = 3.8 \times 10^{29}$ sites m^{-3}.

Once the effective parameters have been obtained, another fitting routine is separately run for the lattice parameters D_0, E_d, K_{s0} and E_s (over 873 K and higher, where the lattice transport has turned to be predominant) and trapping parameters E_t and N_t (over the whole measured temperature range).

It is worth noting that only diffusivity and Sieverts' constant are independently obtained from the experiment, being the activation energies E_d, E_s, correlated with their respective pre-exponentials D_0 and K_{s0}. The permeability Φ is derived from the product of the previous transport parameters, $\Phi = \Phi_0\exp(-E_\Phi/RT) = D_{\mathrm{eff}}K_{s,\mathrm{eff}} = DK_s = D_0K_{s0}\exp[-(E_d+E_s)/RT]$, once the diffusive regime has been checked.

Ebisuzaki et al.'s theory based on the harmonic approximation [18] is used here to analyse the isotope effects in H–W interactions and applied to derive the tritium transport parameters from the H_D and H_P experimental transport data. The variation of H transport parameters in a metal or alloy satisfies the following isotopic laws:

$$\ln\left(\frac{K_{s,\mathrm{eff},\alpha}}{K_{s,\mathrm{eff},\beta}}\right) = 3\left(\frac{f(\theta/\sqrt{\beta}T)}{f(\theta/\sqrt{\alpha}T)}\right) - \frac{3}{2}\ln\left(\frac{\beta}{\alpha}\right) + \frac{g_\alpha^0 - g_\beta^0}{2RT},$$

for the effective Sieverts' constant and

$$\frac{D_{\mathrm{eff},\alpha}}{D_{\mathrm{eff},\beta}} = \sqrt{\frac{\beta}{\alpha}}\left(\frac{f(\theta/\sqrt{\alpha}T)}{f(\theta/\sqrt{\beta}T)}\right)^3\left(\frac{f(\theta^*/\sqrt{\beta}T)}{f(\theta^*/\sqrt{\alpha}T)}\right)^2,$$

for effective diffusivities, α and β being the atomic masses 1, 2, 3 for each isotope H_P, H_D and H_T, g_α^0 and g_β^0 the

molar Gibbs energies of the isotope diatomic gas molecules at the reference state (298 K, 1 bar) [19], and $f(x)$ the vibration partition function defined by $f(x) = \sin h(x/2)/(x/2)$. θ and θ^* are the characteristic vibration temperatures of H_P oscillation in the ground and excited state (i.e., in the bottom of the potential well and the top of the diffusion barrier); they are related to the vibration frequencies v and v^* (s^{-1}) by $\theta = hv/k$ and $\theta^* = hv^*/k$, where h is the Planck constant ($6.6260755 \times 10^{-34}$ J s) and k is the Boltzmann constant (1.380658×10^{-23} J K^{-1}).

5. Results

The effective H_P and H_D Sieverts' constants and effective diffusivities are obtained from modelling the desorption curves. They are depicted in Figs. 5 and 6 together with the resultant fitting regressions and the extrapolated H_T transport parameters. The derived permeabilities are shown in Fig. 7.

The complete set of H_P transport parameters have been calculated as:

$$D\ (\mathrm{m^2\ s^{-1}}) = 5.68 \times 10^{-10} \exp(-9.3/RT),$$
$$K_s\ (\mathrm{mol\ m^{-3}\ Pa^{-1/2}}) = 2.90 \times 10^{-2} \exp(-26.9/RT),$$
$$\Phi\ (\mathrm{mol\ m^{-1}\ Pa^{-1/2}\ s^{-1}}) = 1.65 \times 10^{-11} \exp(-36.2/RT),$$
$$N_t\ (\mathrm{m^{-3}}) = 2.0 \times 10^{23},$$
$$E_t\ (\mathrm{kJ\ mol^{-1}}) = 86.6.$$

The complete set of H_D transport parameters are:

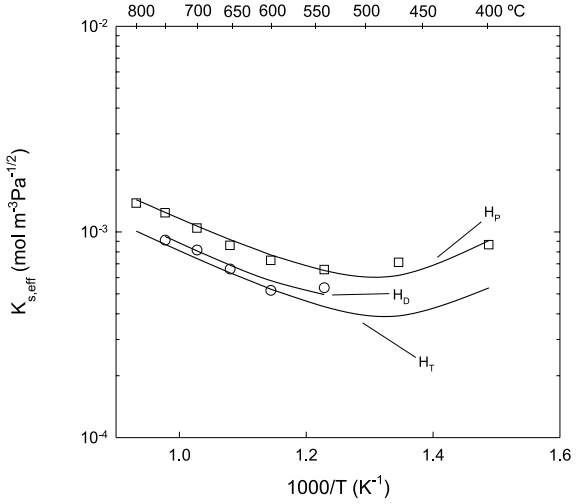

Fig. 5. Arrhenius plot of the Sieverts' constant of the hydrogen isotopes in tungsten. The tritium effective Sieverts' constant has been derived from protium values by applying Ebisuzaki's theory [18].

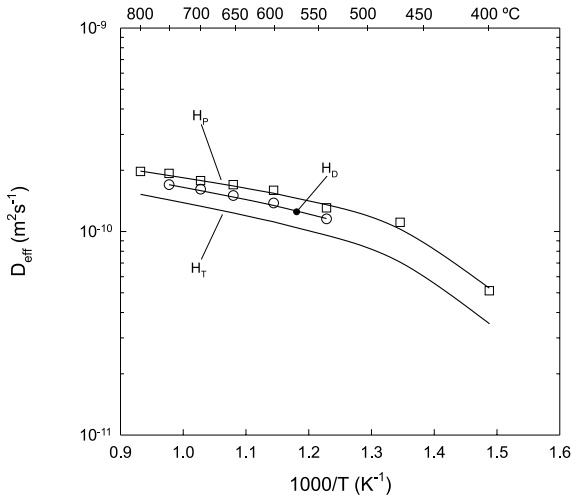

Fig. 6. Arrhenius plot of the effective diffusivity of the hydrogen isotopes in tungsten. The tritium effective diffusivity has been derived from protium values by applying Ebisuzaki's theory [18].

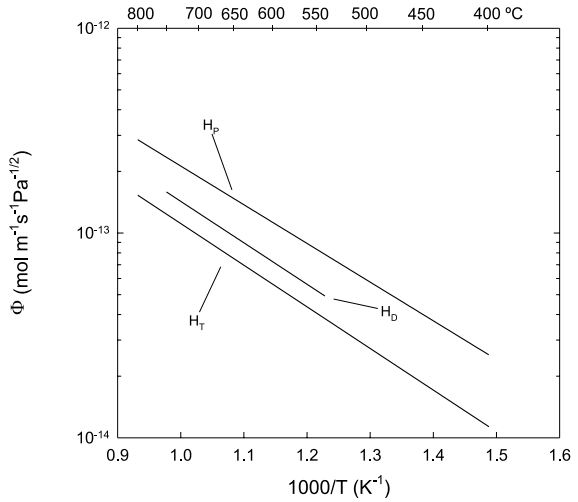

Fig. 7. Arrhenius plot of the permeability of the hydrogen isotopes in tungsten.

$$D\ (\mathrm{m^2\ s^{-1}}) = 5.49 \times 10^{-10} \exp(-10.0/RT),$$
$$K_s\ (\mathrm{mol\ m^{-3}\ Pa^{-1/2}}) = 2.75 \times 10^{-2} \exp(-28.7/RT),$$
$$\Phi\ (\mathrm{mol\ m^{-1}\ Pa^{-1/2}\ s^{-1}}) = 1.51 \times 10^{-11} \exp(-38.7/RT),$$
$$N_t\ (\mathrm{m^{-3}}) = 1.0 \times 10^{23},$$
$$E_t\ (\mathrm{kJ\ mol^{-1}}) = 93.7.$$

The calculated [18] characteristic protium oscillation temperatures are:

$$\theta = 893\ (\pm 178)\ \mathrm{K},$$
$$\theta^* = 2467\ (\pm 227)\ \mathrm{K}.$$

Table 2
Transport parameters of hydrogen isotopes in tungsten amd their corresponding standard deviations (in parenthesis)

	Protium	Deuterium	Tritium
$D_0 \times 10^{10}$ (m^2 s^{-1})	5.68 (±0.04)	5.49 (±0.03)	5.34 (±0.70)
E_d (kJ mol^{-1})	9.3 (±0.6)	10.0 (±0.4)	11.2 (±3.1)
$K_{s0} \times 10^2$ (mol m^{-3} $Pa^{-1/2}$)	2.90 (±0.03)	2.75 (±0.08)	2.25 (±0.40)
E_s (kJ mol^{-1})	26.9 (±1.0)	28.7 (±2.2)	27.8 (±4.1)
$\Phi_0 \times 10^{11}$ (mol m^{-1} $Pa^{-1/2}$ s^{-1})	1.65 (±0.02)	1.51 (±0.04)	1.20 (±0.40)
E_Φ (kJ mol^{-1})	36.2 (±1.7)	38.7 (±2.7)	38.9 (±4.2)
N_t ($\times 10^{-23}$) (sites m^{-3})	2.0 (±1.2)	1.0 (±0.4)	2.3 (±1.9)
E_t (kJ mol^{-1})	86.6 (±23.5)	93.7 (±12.3)	100.5 (±31.3)

The complete set of H_T transport parameters are:

$$D\ (\mathrm{m^2\ s^{-1}}) = 5.34 \times 10^{-10} \exp(-11.2/RT),$$
$$K_s\ (\mathrm{mol\ m^{-3}\ Pa^{-1/2}}) = 2.25 \times 10^{-2} \exp(-27.8/RT),$$
$$\Phi\ (\mathrm{mol\ m^{-1}\ Pa^{-1/2}\ s^{-1}}) = 1.20 \times 10^{-11} \exp(-38.9/RT),$$
$$N_t\ (\mathrm{m^{-3}}) = 2.3 \times 10^{23},$$
$$E_t\ (\mathrm{kJ\ mol^{-1}}) = 100.5.$$

All the activation energies are expressed in kJ mol^{-1} and the ideal gas constant, R, equals 8.314 J K^{-1} mol^{-1}.

The standard deviation obtained for each parameter is tabulated in Table 2 for confidence intervals estimation. The source of errors comes from experimental pressure and temperature deviations (0.08% for pressure and 0.1% for temperature being the reference accuracy for the measuring devices).

6. Discussion

The H atomic dissolution in tungsten (Sieverts' law) is verified (Fig. 8) and the diffusive regime is confirmed because diffusivities measured at the same temperature and different pressures do not depend on pressure (Fig. 9).

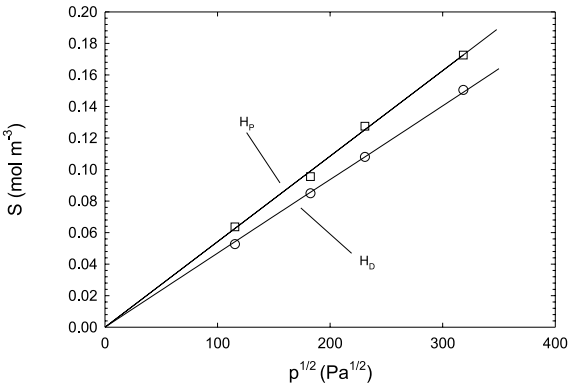

Fig. 8. Solubilities of hydrogen in tungsten at 873 K and different loading pressures. Sieverts' law is fulfilled.

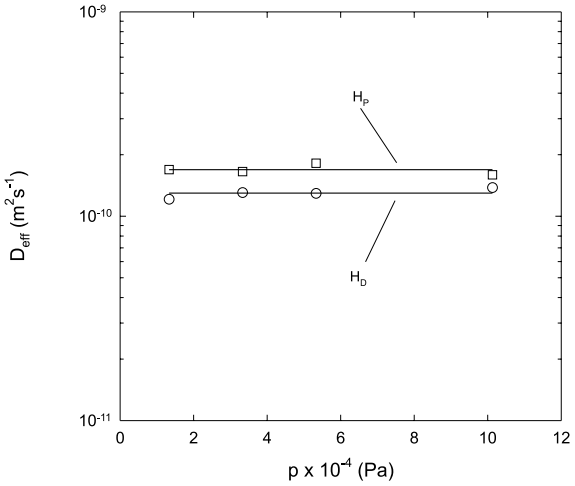

Fig. 9. Effective diffusivities of hydrogen in tungsten at 873 K and different loading pressures. The surface effect is negligible.

Trapping effects on experimental diffusivity and Sieverts' constant values may be noticed (Figs. 5 and 6) below approximately 873 K. The experimental values obtained for the trapping energies (86.6 kJ mol^{-1} for H_P, 93.7 kJ mol^{-1} for H_D) appear to be too high for dislocation or grain boundary traps. However, trapping phenomena with high trapping energies have been previously reported for polycrystalline W [9]. H–H bonding in H clusters nucleated at the structural defects of W was proposed as an explanation for such high trapping energy values. This hypothesis could also explain the results obtained for trapping in the present experiment.

With regard to the isotope effect, a net increase in the effective transport parameters has been noticed when diminishing the mass of the isotope; for effective diffusivity, mean factors $D_{\mathrm{eff}}(H_P)/D_{\mathrm{eff}}(H_D) = 1.13$ (±0.07) and $D_{\mathrm{eff}}(H_D)/D_{\mathrm{eff}}(H_T) = 1.70$ (±0.91) have been evaluated instead of the corresponding classical values 1.41 and 1.22. The fact that the mean increase of effective diffusivity is higher when changing isotope from H_D to H_T than from H_P to H_D may be the consequence of experimental deviations because both confidence

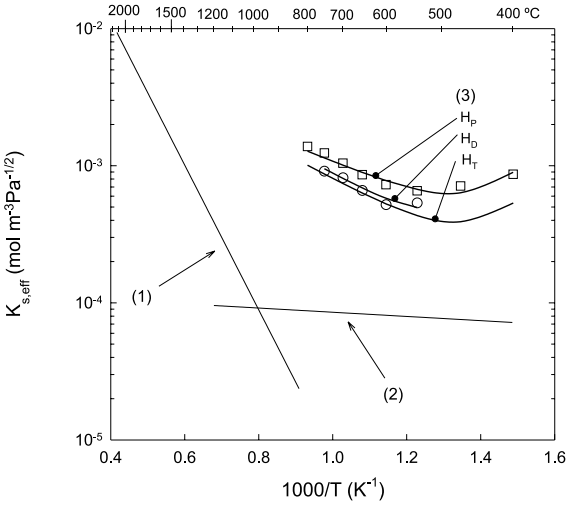

Fig. 10. Effective Sieverts' constant of hydrogen in tungsten: (1) Frauenfelder [3], (2) Zakharov et al. [5], (3) this work.

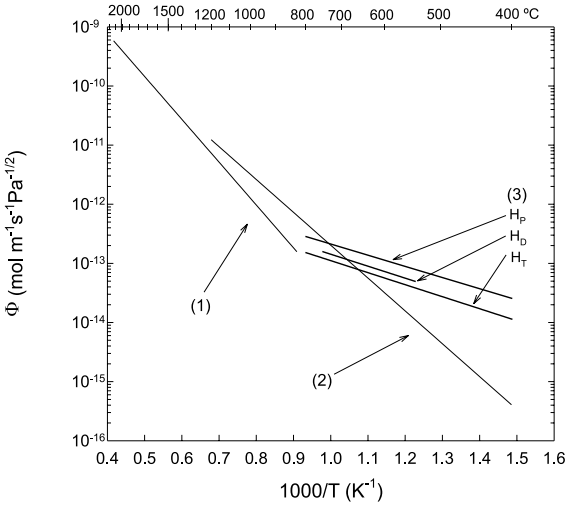

Fig. 12. Permeability of hydrogen in tungsten: (1) Frauenfelder [3], (2) Zakharov et al. [5], (3) this work.

intervals overlap. For effective Sieverts' constant the mean isotopic ratios have been evaluated as $K_{s,eff}(H_P)/K_{s,eff}(H_D) = 1.29\ (\pm 0.09)$ and $K_{s,eff}(H_D)/K_{s,eff}(H_T) = 1.10\ (\pm 0.60)$.

In Figs. 10–12 the obtained diffusive transport parameters are compared with the results reported elsewhere. The broad dispersion existing amongst all the results may be explained as follows. In the experiments using W specimens at high temperatures [3,4,6] the H atomisation phenomenon may imply an underestimation of the evaluated molecular H inventories. Consequently, the transport properties obtained by modelling such molecular inventory may be inaccurate. The experiments using H ion implantation [7,8] to load the W specimens provoke ion-induced traps, so that the effective transport parameters may depart from those obtained only in presence of natural traps. The microstructure of each used specimen may influence the H transport within the bulk of tungsten. Moreover, depending on the manufacturing technique and subsequent heat treatment, the specimens show a particular microstructure with different grain sizes and different dislocation densities; these are sources of internal stress in the material where H may be trapped and even nucleate to form clusters. Other sources of variation may be the non-consideration of temperature transitory periods and long pumping-down stages before the release phase study [3].

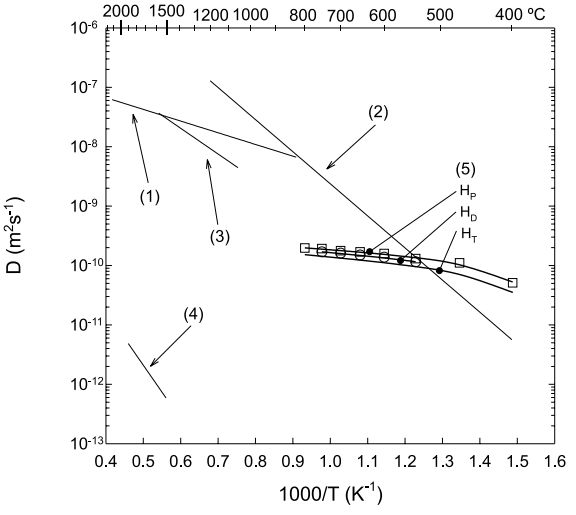

Fig. 11. Effective diffusivity of hydrogen in tungsten: (1) Frauenfelder [3], (2) Zakharov et al. [5], (3) Ryabchikov [6], (4) Moore and Unterwald [4], (5) this work.

In terms of activation energies, the energy of diffusion E_d reported here (9.3 kJ mol^{-1}, H_P, 10.0 kJ mol^{-1}, H_D, 11.2 kJ mol^{-1}, H_T) is the lowest compared to other referenced values. The solution energy evaluated here (26.9 kJ mol^{-1}, H_P, 28.7 kJ mol^{-1}, H_D, 27.8 kJ mol^{-1}, H_T), approximates closer to that reported in [5] rather than the high values obtained in [3,4]. With regard to the trapping effect, the trap density values and the high trapping energies obtained approximate well to the results obtained in [10].

7. Concluding remarks

Hydrogen isotopes transport characteristics in polycrystalline W have been measured using an isovolu-

metric desorption technique. A net reduction in both Sieverts' constant and diffusivity has been noticed as the mass of the isotopes increased. The trapping phenomenon has been noticed below 873 K and the characteristic trapping parameters evaluated. The possibility of H clusters nucleation at structural defects has been identified as the most probable phenomenon explaining the high trapping energies obtained.

References

[1] G. Janeschitz, K. Borrass, G. Federici, Y. Igitkhanov, A. Kukushkin, H.D. Pacher, G.W. Pacher, M. Sugihara, J. Nucl. Mater. 220–222 (1995) 73.
[2] J.W. Davis, V.R. Barabash, A. Makhanov, L. Plöchl, K.T. Slattery, J. Nucl. Mater. 258–263 (1998) 308.
[3] J. Frauenfelder, J. Vac. Sci. Technol. 6 (1968) 388.
[4] G.E. Moore, F.C. Unterwald, J. Chem. Phys. 40 (1964) 2639.
[5] A.P. Zakharov, V.M. Sharapov, E.I. Evko, Sov. Mater. Sci. 9 (1973) 149.
[6] L.N. Ryabchikov, Ukr. Fiz. Zh. 9 (1964) 293.
[7] P. Franzen, C. García Rosales, H. Plank, V.Kh. Alimov, J. Nucl. Mater. 241–243 (1997) 1082.
[8] A.A. Pisarev, A.V. Varava, S.K. Zhdanov, J. Nucl. Mater. 220–222 (1995) 926.
[9] R.A. Anderl, D.F. Holland, G.R. Longhurst, R.J. Pawelko, C.L. Trybus, C.H. Sellers, Fus. Technol. 21 (1992) 745.
[10] S. Alberici, A. Perujo, J. Camposilvan, Fus. Technol. 28 (1995) 1108.
[11] S. Tominetti, M. Caorlin, J. Camposilvan, A. Perujo, F. Reiter, J. Nucl. Mater. 176&177 (1990) 672.
[12] G.A. Esteban, A. Perujo, K. Douglas, L.A. Sedano, J. Nucl. Mater. 281 (2000) 34.
[13] L.A. Sedano, A. Perujo, C.H. Wu, J. Nucl. Mater. 273 (1999) 285.
[14] L.A. Sedano, in: Obtaining H Interaction Parameters for Carbon Fibre Composites by Modelling Isovolumetric Desorption Experiments, Euro-report: EUR 17320 EN, 1997.
[15] R.A. Oriani, Acta Metall. 18 (1970) 147.
[16] E. Serra, A. Perujo, G. Benamati, J. Nucl. Mater. 245 (1997) 285.
[17] A. Seeger, Phys. Lett. 58A (1976) 137.
[18] Y. Ebisuzaki, W.J. Kass, M. O'Keeffe, J. Chem. Phys. 46 (1967) 1373.
[19] L. Haar, A.S. Friedman, in: Ideal gas thermodynamic functions and isotope exchange functions for the diatomic hydrides, deuterides, and tritides, US Department of Commerce, National Bureau of Standards, 1961.